Applied Mathematics & Information Sciences
An International Journal

http://dx.doi.org/10.12785/amis/080323

Influence of Lateral Walls on Peristaltic Flow of a Couple Stress Fluid in a Non-Uniform Rectangular Duct

Safia Akram[1,*], *Kh. S. Mekheimer*[2,3] *and S. Nadeem*[4]

[1] Department of Basic Sciences, MCS, National University of Sciences and Technology, Rawalpindi 46000, Pakistan
[2] Faculty of Science, Mathematics & Statistic Department, Taif University, Hawia(888) Taif, Saudi Arabia
[3] Faculty of Science (Men), Mathematical Department, Al-Azhar University, Nasr City, Cairo, Egypt
[4] Department of Mathematics, Quaid-i-Azam University 45320, Islamabad 44000, Pakistan

Received: 25 May. 2013, Revised: 29 Sep. 2013, Accepted: 30 Sep. 2013
Published online: 1 May. 2014

Abstract: In the present investigation we have studied the peristaltic flow of a couple stress fluid in a non-uniform rectangular duct. The flow is investigated in a wave frame of reference moving with the velocity c away from the fixed frame. The peristaltic waves propagating on the horizontal side walls of a non-uniform rectangular duct is studied under lubrication approach. The exact solutions of velocity and pressure gradient have been found under lubrication approach. The pumping characteristics, axial pressure gradient, velocity field and trapping phenomena have been discussed to highlight the physical features of emerging parameters of couple stress fluid.

Keywords: Peristaltic flow, non-uniform rectangular duct, couple stress fluid, exact solution

1 Introduction

The peristaltic flows of Newtonian and non-Newtonian fluids have achieved special status due to its wide range of applications in physiology, industry and biomedical sciences [1,2,3]. The authors have taken various kind of geometries in peristaltic flows such as uniform and nonuniform channels and tubes, peristaltic flows in endoscope, planner channel, symmetric and asymmetric channels. De Vries et al [4] and Chalubinski et al [5], experimentally shared that the flow due to myometrial contractions, intrauterine fluid is peristaltic type motion and myometrial contractions may occurs in both symmetric and asymmetric channel. Later on , Eytan and Elad [6] have made a mathematical model which discussed the peristaltic fluid flow in a two dimensional channel with wave trains having a phase difference moving independently on the upper and lower walls to simulate intra-uterine fluid motion in a sagital cross section of the uterus. Only a limited attention have been focused to the study of peristaltic flows of non-Newtonian fluids in asymmetric channel. Mention may be made to the interesting works of [7,8,9,10,11,12]. Recently, Reddy et al [13] have examined the peristaltic flows in a rectangular duct. According to them [13], the sagittal cross section of the uterus may be better approximated by a tube of rectangular cross section than a two dimensional flow. They [13] have considered a viscous fluid in a rectangular channel and found the exact solution with the help of separation of variables under the long wavelength approximation. The idea of [13] have been extended by Mandviwalla and Archer [14] and considered the influence of slip boundary condition on peristaltic pumping in a rectangular channel. Nadeem and Akram [15] has examined the peristaltic flow of Jeffrey fluid in a rectangular channel. Very recently, Mekheimer et al [16] have examined the effect of lateral walls on peristaltic flow through an asymmetric rectangular duct.

The objective of the present investigation is to discuss the peristaltic flow of couple stress fluid model in a non-uniform rectangular duct by introducing the lateral walls separated by a distance 2h in a channel of height 2a. The closed form solutions of the modelled equations of couple stress fluid in a non-uniform rectangular channel has been presented under the long wave length approximation. The physical features of various parameters have been discussed through graphs. A

* Corresponding author e-mail: safia_akram@yahoomail.com

comparison of our solution and the available results are presented. Finally, the stream lines are also shown.

Nomenclature

U,V	velocity components in X and Y directions in fixed frame
u,v	velocity components in x and y directions in wave frame
ρ	constant velocity
Re	Reynolds number
β	aspect ratio
λ	wave length
c	velocity of propagation
Q	volume flow rate
δ	long wave length
Ψ	stream function
S	extra stress tensor
γ	couple stress parameter

2 Mathematical Formulation

Let us consider the peristaltic flow of an incompressible couple stress fluid in a duct of rectangular cross section having the channel width 2d and height 2a. We are considering the Cartesian coordinates system in such a way that $X-axis$ is taken along the axial direction, $Y-axis$ is taken along the lateral direction and $Z-axis$ is along the vertical direction of a rectangular duct.

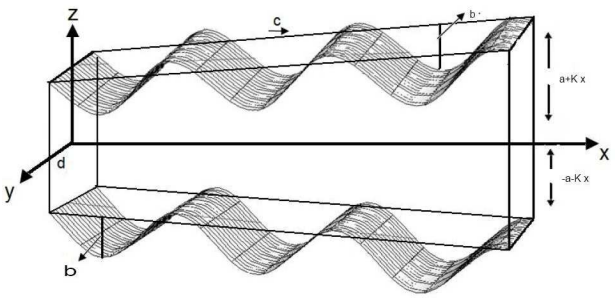

Fig. 1: Geometry of the problem

The peristaltic waves on the walls are represented as

$$Z = H(X,t) = \pm a \pm kx \pm b\sin\left[\frac{2\pi}{\lambda}(X-ct)\right], \quad (1)$$

where a and b are the amplitudes of the waves, λ is the wave length, c is the velocity of propagation, t is the time and X is the direction of wave propagation. The walls parallel to XZ plane remain undisturbed and are not subject to any peristaltic wave motion. We assume that the lateral velocity is zero as there is no change in lateral direction of the duct cross section. Let $(U,0,W)$ be the velocity for a rectangular duct. The governing equations for the flow problem are

$$\frac{\partial U}{\partial X} + \frac{\partial W}{\partial Z} = 0, \quad (2)$$

$$\rho\left(\frac{\partial U}{\partial t} + U\frac{\partial U}{\partial X} + W\frac{\partial U}{\partial Z}\right) = -\frac{\partial P}{\partial X} + \mu\left(\frac{\partial^2 U}{\partial X^2} + \frac{\partial^2 U}{\partial Y^2} + \frac{\partial^2 U}{\partial Z^2}\right) - \eta\left(\frac{\partial^4 U}{\partial X^4} + \frac{\partial^4 U}{\partial Y^4} + \frac{\partial^4 U}{\partial Z^4} + 2\frac{\partial^4 U}{\partial X^2 \partial Y^2} + 2\frac{\partial^4 U}{\partial X^2 \partial Z^2} + 2\frac{\partial^4 U}{\partial Y^2 \partial Z^2}\right), \quad (3)$$

$$0 = -\frac{\partial P}{\partial Y}, \quad (4)$$

$$\rho\left(\frac{\partial W}{\partial t} + U\frac{\partial W}{\partial X} + W\frac{\partial W}{\partial Z}\right) = -\frac{\partial P}{\partial Z} + \mu\left(\frac{\partial^2 W}{\partial X^2} + \frac{\partial^2 W}{\partial Y^2} + \frac{\partial^2 W}{\partial Z^2}\right) - \eta\left(\frac{\partial^4 W}{\partial X^4} + \frac{\partial^4 W}{\partial Y^4} + \frac{\partial^4 W}{\partial Z^4} + 2\frac{\partial^4 W}{\partial X^2 \partial Y^2} + 2\frac{\partial^4 W}{\partial X^2 \partial Z^2} + 2\frac{\partial^4 W}{\partial Y^2 \partial Z^2}\right), \quad (5)$$

in which ρ is the density, P is the pressure and t is the time.

Let us define a wave frame (x,y) moving with the velocity c away from the fixed frame (X,Y) by the transformation

$$x = X - ct, y = Y, \ z = Z, \ u = U - c, \quad w = W, \ p(x,z) = P(X,Z,t). \quad (6)$$

Defining the following non-dimensional quantities

$$\bar{x} = \frac{x}{\lambda}, \bar{y} = \frac{y}{d}, \bar{z} = \frac{z}{a}, \bar{u} = \frac{u}{c}, \bar{w} = \frac{w}{c\delta}, \bar{t} = \frac{ct}{\lambda}, h = \frac{H}{a}, \bar{p} = \frac{a^2 p}{\mu c \lambda}, \Re e = \frac{\rho a c \delta}{\mu},$$

$$\beta = \frac{a}{d}, \delta = \frac{a}{\lambda}, \gamma = \sqrt{\frac{\mu}{\eta}}a. \quad (7)$$

Using the above non-dimensional quantities in Eqs. (2) to (5), the resulting equations after dropping the bars can be written as

$$\frac{\partial u}{\partial x} + \frac{\partial w}{\partial z} = 0, \quad (8)$$

$$\Re e\left(u\frac{\partial u}{\partial x} + w\frac{\partial u}{\partial z}\right) = -\frac{\partial p}{\partial x} + \delta^2\frac{\partial^2 u}{\partial x^2} + \beta^2\frac{\partial^2 u}{\partial y^2} + \frac{\partial^2 u}{\partial z^2} - \frac{1}{\gamma^2}\left(\delta^4\frac{\partial^4 u}{\partial x^4} + \beta^4\frac{\partial^4 u}{\partial y^4} + \frac{\partial^4 u}{\partial z^4} + 2\delta^2\beta^2\frac{\partial^4 u}{\partial x^2 \partial y^2} + 2\delta^2\frac{\partial^4 u}{\partial x^2 \partial z^2} + 2\beta^2\frac{\partial^4 u}{\partial y^2 \partial z^2}\right), \quad (9)$$

$$0 = -\frac{\partial p}{\partial y}, \quad (10)$$

$$\Re e\delta^2\left(u\frac{\partial w}{\partial x} + w\frac{\partial w}{\partial z}\right) = -\frac{\partial p}{\partial z} + \delta^2\left(\left(\delta^2\frac{\partial^2 w}{\partial x^2} + \beta^2\frac{\partial^2 w}{\partial y^2} + \frac{\partial^2 w}{\partial z^2}\right) - \frac{1}{\gamma^2}\left(\delta^6\frac{\partial^4 w}{\partial x^4} + \delta^2\beta^4\frac{\partial^4 w}{\partial y^4} + \delta^2\frac{\partial^4 w}{\partial z^4} + 2\delta^4\beta^2\frac{\partial^4 w}{\partial x^2 \partial y^2} + 2\delta^4\frac{\partial^4 w}{\partial x^2 \partial z^2} + 2\delta^2\beta^2\frac{\partial^4 w}{\partial y^2 \partial z^2}\right), \quad (11)$$

Under the assumption of long wave length $\delta \leq 1$ and low Reynolds, neglecting the terms of order δ and higher, Eqs. (8) to (12) take the form

$$\frac{dp}{dx} = \beta^2\frac{\partial^2 u}{\partial y^2} + \frac{\partial^2 u}{\partial z^2} - \frac{1}{\gamma^2}\left(\beta^4\frac{\partial^4 u}{\partial y^4} + \frac{\partial^4 u}{\partial z^4} + 2\beta^2\frac{\partial^4 u}{\partial y^2 \partial z^2}\right), \quad (12)$$

$$\frac{\partial u}{\partial x} + \frac{\partial w}{\partial z} = 0. \quad (13)$$

The corresponding boundary conditions are

$$u = -1 \text{ at } y = \pm 1, \ \frac{\partial^2 u}{\partial y^2} = 0 \text{ at } y = \pm 1, \quad (14)$$

$$u = -1 \text{ at } z = \pm h(x) = \pm 1 \pm Kx \pm \phi\sin 2\pi x, \ \frac{\partial^2 u}{\partial z^2} = 0 \text{ at } z = \pm h(x), \quad (15)$$

where $0 \leq \phi \leq 1$, $\phi = 0$ for straight duct, $\phi = 1$ corresponds to total occlusion and $K = \frac{\lambda k}{a(k<<1)}$.

3 Expressions for different wave shape

The expression for the triangular, square and trapezoidal wave are derived from the Fourier series. In this analysis total number of terms in the series that are incorporated are 50.

1.Triangular wave

$$h(x)=1+Kx+\phi\left[\frac{8}{\pi^3}\sum_{m=1}^{\infty}\frac{(-1)^{m+1}}{(2m-1)^2}\sin(2\pi(2m-1)x)\right],$$

2.Trapezoidal wave

$$h(x)=1+Kx+\phi\left[\frac{32}{\pi^2}\sum_{m=1}^{\infty}\frac{\sin\frac{\pi}{8}(2m-1)}{(2m-1)^2}\sin(2\pi(2m-1)x)\right],$$

3.Square wave

$$h_1(x)=1+Kx+\phi\left[\frac{4}{\pi}\sum_{m=1}^{\infty}\frac{(-1)^{m+1}}{(2m-1)}\cos(2(2m-1)\pi x)\right],$$

4 Solution of the problem

The closed form solution of Eq. (12) satisfying the boundary conditions (14) and (15) can be directly written as

$$u=-1+\frac{1}{2}\frac{dp}{dx}\left(-h^2(x)+z^2+\frac{2}{\gamma^2}\right)-\frac{dp}{dx}\left(\frac{\cosh[z\gamma]\,\mathrm{sech}[h\gamma]}{\gamma^2}\right)+2\frac{dp}{dx}h^2(x)\sum_{n=1}^{\infty}\frac{(-1)^n\cosh(\alpha_n y/\beta h(x))\cos(\alpha_n z/h(x))}{\alpha_n^3\cosh(\alpha_n/\beta h(x))}, \quad (16)$$

where $\alpha_n=(2n-1)\pi/2$

The volumetric flow rate is given by

$$q=\int_0^1\int_0^{h(x)}u\,dydz=-h(x)-\frac{h^3(x)}{3}\frac{dp}{dx}\left\{1-\frac{3}{\gamma^2h^2(x)}+\frac{3\,\mathrm{sech}[h\gamma]\sinh[h\gamma]}{\gamma^3h^3(x)}-6\beta h(x)\sum_{n=1}^{\infty}\frac{1}{\alpha_n^5}\tanh(\alpha_n/\beta h(x))\right\}. \quad (17)$$

The instantaneous flux is defined as

$$\bar{Q}=\int_0^1\int_0^{h(x)}(u+1)\,dydz=q+h(x). \quad (18)$$

The average volume flow rate over one period $\left(T=\frac{\lambda}{c}\right)$ of the peristaltic wave is defined as

$$Q=\frac{1}{T}\int_0^T\bar{Q}dt=q+1. \quad (19)$$

The pressure gradient is obtained from Eq. (17) and (19) as

$$\frac{dp}{dx}=\frac{-3(Q-1+h(x))}{h^3(x)\left(1-\frac{3}{\gamma^2h^2(x)}+\frac{3\,\mathrm{sech}[h\gamma]\sinh[h\gamma]}{\gamma^3h^3(x)}-6\beta h(x)\sum_{n=1}^{\infty}\frac{1}{\alpha_n^5}\tanh(\alpha_n/\beta h(x))\right)}. \quad (20)$$

Integration of Eq. (20) over one wavelength yields

$$\Delta p=\int_0^1\frac{dp}{dx}dx. \quad (21)$$

Special Case

It is noticed here that when $K\longrightarrow 0$ and $\gamma\to\infty$ the solutions of Reddy et al [13] $u=-1-\frac{h^2(x)}{2}\frac{dp}{dx}\left\{1-\frac{z^2}{h^2(x)}-4\sum_{n=1}^{\infty}\frac{(-1)^n\cosh(\alpha_n y/\beta h(x))\cos(\alpha_n z/h(x))}{\alpha_n^3\cosh(\alpha_n/\beta h(x))}\right\}$, is recovered as a special case of our problem.

5 Numerical Results and Discussion

This section deals with the graphical results of the problem under consideration. The expression for the pressure rise and pressure gradient is calculated using a mathematics soft ware Mathematica because expression 20 and 21 are not integrable in closed form. So numerical integrations are performed and the graphical results are presented. Fig. 2 depicts the variation of pressure rise with volume flow rate Q for different values of aspect ratio β. It is scrutinized from Fig. 2 that any two pumping curves interconnect at a point in the 3^{rd} quadrant. As long as this point remain in the 3rd quadrant, to the left of this point both peristaltic pumping and retrograde pumping increases and to the right both pumping and free pumping decreases with an increase in β. The variation of pressure rise Δp with volume flow rate Q for different values of couple stress parameters γ and K is demonstrated in Figs. 3 and 4. It is depicted from Fig. 3 and 4 that the behavior of pressure rise in case of γ and K is quite opposite as compared with β.

In order to see the bahvior of pressure gradient for different values of aspect ratio β, couple stress parameter γ, volume flow rate Q and non-uniform channel parameter K against x, Figs. 5 to 8 is presented. It is observed that pressure gradient decreases with an increase in β and K and increases with an increase in γ and Q. The velocity profile for different values of Q, γ and β are shown in Figs. 9 to 11. It is observed that the velocity profile increases with an increases in volume flow rate Q and aspect ratio β and decreases with an increase in couple stress parameter γ.

Trapping Phenomena

The stream lines in general in the wave frame have a contour similar to the walls as the walls are immobile. To enclose a bolus of fluid particles in closed stream lines, some streamlines split due to the subsistence of a stagnation point under certain conditions. Figs. 12 to 15 show the stream lines for different values of β, γ, Q and K. It is observed from Fig. 12 and 13 that the size of the trapping bolus decreases with an increase in aspect ratio β and couple stress parameter γ. From Fig. 14 it is observed that the size and number of the trapping bolus increases with an increase in volume flow rate Q. Stram lines for different values of K are shown in Fig. 15. It is depicted that the number of the trapping bolus reduces with an increase in K. Fig. 16 shows the stream lines for different wave forms.

The results of pressure rise for different values of aspect ratio β, and amplitude ratio ϕ are tabulated in tables 1 to 2. It is observed from the tables 1 and 2 that with an increase in aspect ratio β and amplitude ratio ϕ the pressure rise increases. The results of velocity field against different values of volume flow rate Q and aspect ratio β are tabulated in tables 3 and 4. It is observed from the tables that the velocity profile increases with an increases in volume flow rate Q and aspect ratio β.

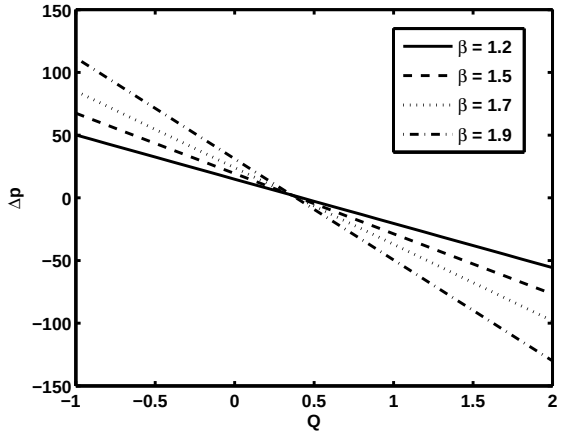

Fig. 2: Variation of Δp with Q for different values of β at $\phi = 0.6$ and $\gamma = 5$, $K = 0.005$.

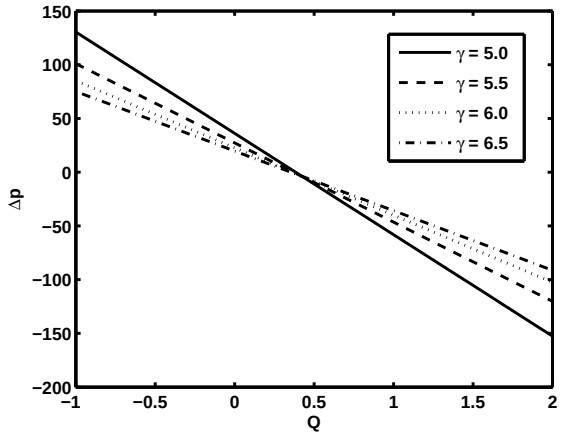

Fig. 3: Variation of Δp with Q for different values of γ at $\phi = 0.6$ and $\beta = 2$, $K = 0.005$.

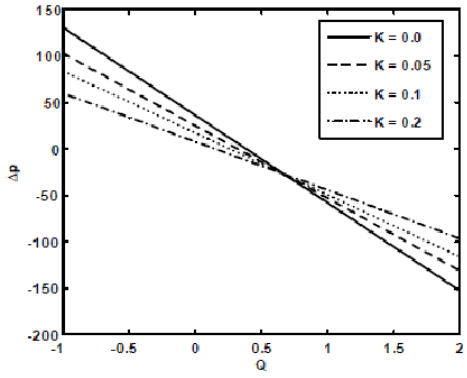

Fig. 4: Variation of Δp with Q for different values of K at $\phi = 0.6$ and $\beta = 2$, $\gamma = 5$.

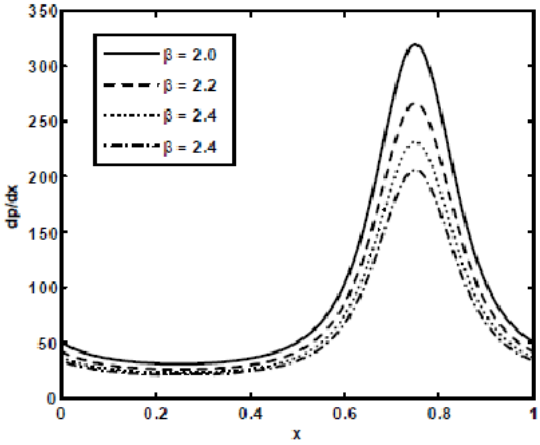

Fig. 5: Variation of dp/dx with x for different values of β at $Q = 2$, $\gamma = 2.5$ and $\phi = 0.6$, $K = 0.005$.

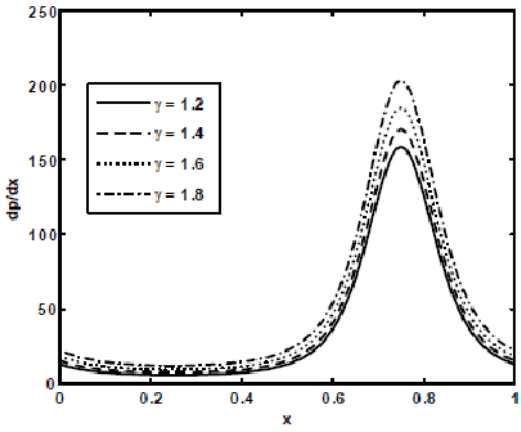

Fig. 6: Variation of dp/dx with x for different values of γ at $Q = 2$, $\beta = 2$ and $\phi = 0.6$, $K = 0.005$.

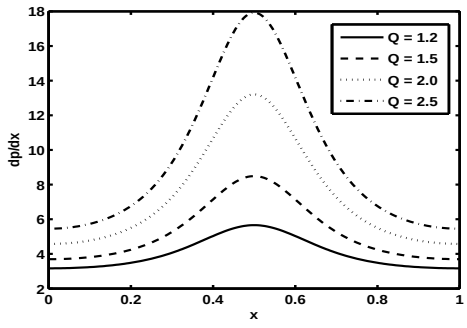

Fig. 7: Variation of dp/dx with x for different values of Q at $\beta = 2$, $\gamma = 2$ and $\phi = 0.6$, $K = 0.005$.

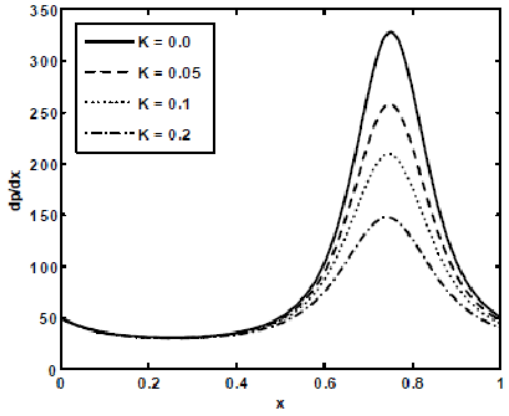

Fig. 8: Variation of dp/dx with x for different values of K at $\beta = 2$, $\gamma = 2$ and $\phi = 0.6$, $Q = 2$.

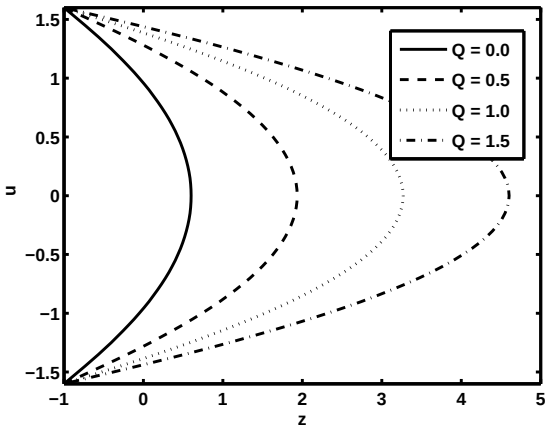

Fig. 9: Velocity profile for different values of Q for fixed $y = 0.5$,$x = 0$, $\beta = 0.5$, $\phi = 0.6$, $\gamma = 8$, $K = 0.005$.

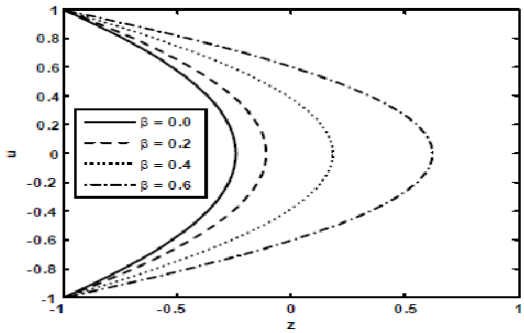

Fig. 10: Velocity profile for different values of β for fixed $y = 0.5$,$x = 0$, $Q = 0.5$, $\phi = 0.6$, $\gamma = 8$, $K = 0.005$.

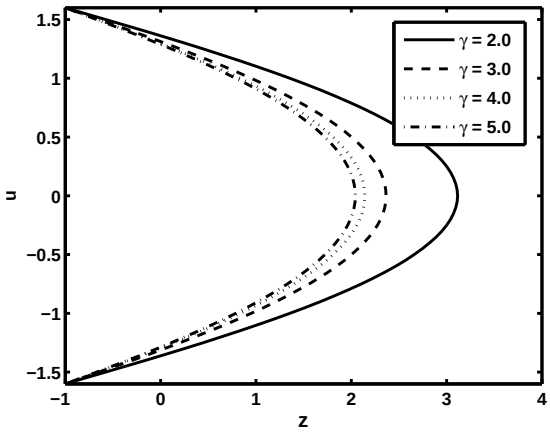

Fig. 11: Velocity profile for different values of γ for fixed $y = 0.5$,$x = 0$, $Q = 0.5$, $\phi = 0.6$, $\beta = 0.5$, $K = 0.005$.

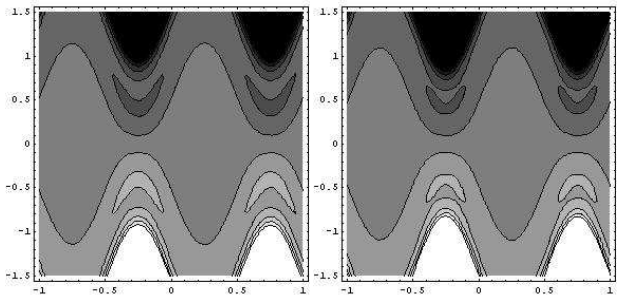

Fig. 12: Stream lines for different values of β. Fig. a (for $\beta = 5$), Fig. b (for $\beta = 3$). The other parameters are $Q = 0.8$, $y = 0.5$, $\phi = 0.6$, $\gamma = 3.0$, $K = 0.005$.

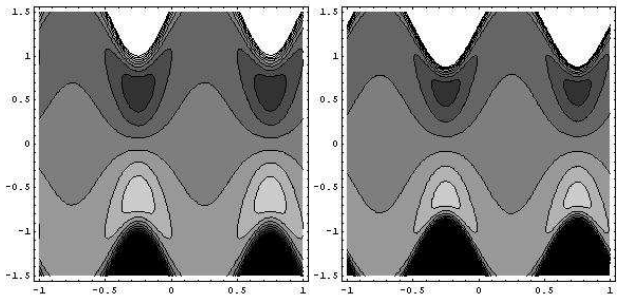

Fig. 13: Stream lines for different values of γ. Fig. a (for $\gamma = 5$), Fig. b (for $\gamma = 10$), The other parameters are $\beta = 2$, $y = 0.5$, $\phi = 0.6$, $Q = 0.6$, $K = 0.005$.

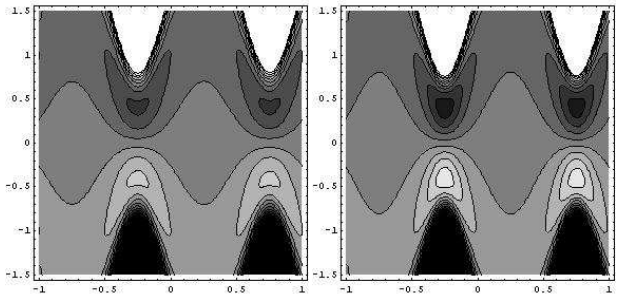

Fig. 14: Stream lines for different values of Q. Fig. a (for $Q = 0.8$), Fig. b (for $Q = 1.0$), The other parameters are $\beta = 1$, $y = 0.5$, $\phi = 0.6$, $\gamma = 3.0$, $K = 0.005$.

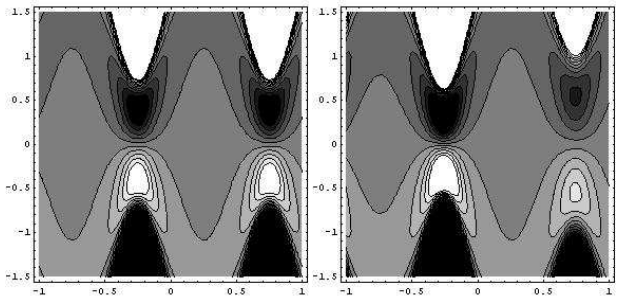

Fig. 15: Stream lines for different values of K. Fig. a (for $K = 0.0$), Fig. b for ($K = 0.2$), The other parameters are $\beta = 0.5$, $y = 0.5$, $\phi = 0.6$, $\gamma = 3.0$, $Q = 2$.

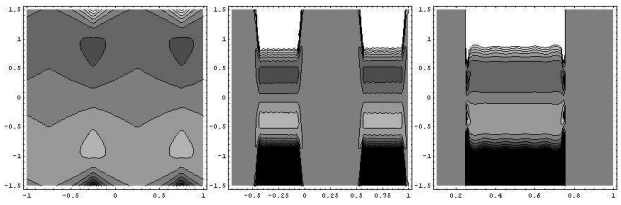

a b c

Fig. 16: Stream lines for wave forms Fig. (a) triangular wave, Fig. (b) trapezoidal wave, Fig. (c) sqaure wave. The other parameters are $\beta = 1$, $y = 0.5$, $\phi = 0.6$, $Q = 3$, $K = 0.005$, $\gamma = 3.0$.

Table 1: Variation of pressure rise for various values of β (aspect ratio) for fixed $\phi = 0.6$ and $\gamma = 5$

Q	Δp for $\beta = 0$ (2-dimensional channel)	Δp for $\beta = 0.5$	Δp for $\beta = 1$ (rectangular duct becomes square duct)	Δp for $\beta = 2$
-0.1	8.78166	11.1436	15.1987	43.981
0	7.25912	9.15148	12.3207	34.7449
0.1	5.73658	7.15934	9.44269	25.5087
0.2	4.21404	5.1672	6.56466	16.2726
0.3	2.6915	3.17505	3.68664	7.03645
0.4	1.16896	1.18291	0.808621	-2.1997
0.5	-0.353583	-0.809236	-2.0694	-11.4359

Table 2: Variation of pressure rise for various values of ϕ for fixed $\beta = 2$ and $\gamma = 6$.

Q	Δp for $\phi = 0$ (Poiseuille flow)	Δp for $\phi = 0.2$	Δp for $\phi = 0.4$	Δp for $\phi = 0.6$	Δp for $\phi = 0.8$
-0.1	3.8575	5.51272	12.722	43.981	764.346
0	-0.0987672	1.32261	7.53677	34.7449	673.927
0.1	-4.05503	-2.86749	2.35157	25.5087	583.507
0.2	-8.01129	-7.05759	-2.83362	16.2726	493.088
0.3	-11.9676	-11.2477	-8.01882	7.03645	402.669
0.4	-15.9238	-15.4378	-13.204	-2.1997	312.25
0.5	-19.8801	-19.6279	-18.3892	-11.4359	221.831

Table 3: Velocity for various values of Q for fixed $y = 0.5$,$x = 0$, $\beta = 2$, $\phi = 0.6$, $\gamma = 8$.

z	u(x,y,z) for $Q = 0.0$	u(x,y,z) for $Q = 0.5$	u(x,y,z) for $Q = 1.0$	u(x,y,z) for $Q = 1.5$
-1	-1	-1	-1	-1
-0.8	-0.811928	-0.52982	-0.0596394	0.410541
-0.6	-0.655058	-0.137645	0.72471	1.58707
-0.4	-0.53963	0.150926	1.30185	2.45278
-0.2	-0.469297	0.326759	1.65352	2.98028,
0	-0.445687	0.385782	1.77156	3.15735
0.2	-0.469297	0.326759	1.65352	2.98028
0.4	-0.53963	0.150926	1.30185	2.45278
0.6	-0.655058	-0.137645	0.72471	1.58707
0.8	-0.811928	-0.52982	-0.0596394	0.410541
1	-1	-1	-1	-1

Table 4: Velocity for various values of β for fixed $y = 0.5$,$x = 0$, $Q = 0.5$, $\phi = 0.6$, $\gamma = 8$.

Q	u(x,y,z) for $\beta = 0$ (2-dimensional channel)	u(x,y,z) for $\beta = 0.5$	u(x,y,z) for $\beta = 1$ (rectangular duct becomes square duct)	u(x,y,z) for $\beta = 2$
-1	-1	-1	-1	-1
-0.8	-0.737958	-0.52982	-0.00211011	2.48466
-0.6	-0.522914	-0.137645	0.83942	5.41223
-0.4	-0.367293	0.150926	1.46395	7.57172
-0.2	-0.273603,	0.326759	1.84626	8.88682
0	-0.242346	0.385782	1.97484	9.32804
0.2	-0.273603	0.326759	1.84626	8.88682
0.4	-0.367293	0.150926	1.46395	7.57172
0.6	-0.522914	-0.137645	0.83942	5.41223
0.8	-0.737958	-0.52982	-0.00211011	2.48466
1	-1	-1	-1	-1

References

[1] Abd El Hakeem Abd El Naby, A. E. M. El Misery and M. F. Abd El Kareem, Separation in the fow through peristaltic motion of a carreau fluid in uniform tube, Phys. A., **343**, 1-14 (2004).

[2] A. Ramachandra Rao and Manoranjan Mishra, Peristaltic transport of a power-law fluid in a porous tube, J. Non-Newtonian Fluid Mech., **121**, 163-174 (2004).

[3] M. H. Haroun, Effect of Deborah number and phase difference on peristaltic transport of a third-order fluid in an asymmetric channel, Commun. Nonlinear Sci. Numer. Simulat., **12**, 1464-1480 (2007).

[4] K. De. Vries, E. A. Lyons, J. Ballard, C. S. Levi and D. J. Linday, Contraction of the inner third of myometrium, Am. J. Obstet. Gynecol, **162**, 679-682 (1990).

[5] K. Chalubinski, J. Deutinger and G. Bernaschek, Vaginosonography for recording of cycle-related myometrial contractions, Fertill. Steril., **59**, 225-228 (1993).

[6] O. Eytan and D. Elad, Analysis of intra-uterine fluid motion induced by uterine contractions, Bull. Math. Biol., **61**, 221 (1999).

[7] S. Nadeem and Safia Akram, Influence of inclined magnetic field on peristaltic flow of a Jeffrey fluid with heat and mass transfer in an inclined symmetric or asymmetric channel, Asia Pacific J.chem. Eng., **7**, 33-44 (2012).
[8] A. Afsar Khan, R. Ellahi and K. Vafai**,** Peristaltic Transport of a Jeffrey Fluid with Variable Viscosity through a Porous Medium in an Asymmetric Channel, Advan. Math. Phys.**,** Article ID 169642, 15 pages, (2012).
[9] Safia Akram and S. Nadeem, Simulation of heat and mass transfer on peristaltic flow of hyperbolic tangent fluid in an asymmetric channel, Inter. J. Num. methods in fluids., **70**, 1475-1493 (2012).
[10] Ambreen Afsar Khan**,** R. Ellahi and M. Usman, The Effects of variable viscosity on the peristaltic flow of non-Newtonian fluid through a porous medium in an inclined channel with slip conditions, J. Porous Media, **16**, 59-67 (2013).
[11] Safia Akram and S. Nadeem, Numerical and analytical solutions of peristaltic transport of a six constant Jeffreys model of Fluid in a symmetric or asymmetric channel, Inter. J. fluid Mech. Research, **39**, 238-260 (2012).
[12] Safia Akram, Abdul Ghafoor and S. Nadeem, Mixed convective heat and Mass transfer on a peristaltic flow of a non-Newtonian fluid in a vertical asymmetric channel, Heat Trans. Asian Research, **41**, 613-633 (2012).
[13] M. V. Subba Reddy, M. Mishra, S. Sreenadh and A. Ramachandra Rao, Influence of lateral walls on peristaltic flow in a rectangular duct, J. fluids Engineering.
[14] X. Mandviwalla and R. Archer, The influence of slip boundary conditions on peristaltic pumping in a rectangular channel, J. fluids Engineering.
[15] S. Nadeem and Safia Akram, Peristaltic flow of a Jeffrey fluid in a rectangular duct, Nonlinear Analy. real world appl., **11**, 4238-4247 (2010).
[16] Kh. S. Mekheimera, S. Z.-A. Husseny and A. I. Abd el Lateef, Effect of lateral walls on peristaltic flow through an asymmetric rectangular duct, Appl. Bionics and Biomechanics.

Safia Akram ia an Assistant Professor at National University of Sciences and technology, (MCS), Islamabad. Her field of research is applied mathematics and computationl fluid mechanics. She is recipient of research productive award in year 2010-2011 and 2011 to 2012 by Pakistan Council for Science and Technology. Her research articles have been published in international journals.

Kh. S. Mekheimer is a Professor of Mathematics at Al-Azhar University, Cairo, EGYPT. His field of research is Biofluidmechanics, Magnetohydrodynamic, Porous medium, Two-phase flows and Physiological flows (blood flow), Flow in organs. He is recipient of best scientific citation prize, 2013, Taif University, KSA. He is also an author of books and editor of international journals.

Sohail Nadeem is an Associate Professor at Quaid-i-Azam University Islamabad. He is recipient of Razi-ud-Din gold medal by Pakistan Academy of Sciences and Tamgha-i-Imtiaz by the President of Pakistan. He is young fellow of TWAS, Italy